Multiconfigurational-Dirac-Fock calculation of the $2s^2\ ^1S_0$–$2s2p\ ^3P_1$ spin-forbidden transition for the Be-like isoelectronic sequence

Anders Ynnerman* and Charlotte Froese Fischer†
Computer Science Department, Vanderbilt University, Nashville, Tennessee 37235
(Received 30 August 1994)

Accurate *ab initio* multiconfigurational Dirac-Fock (MCDF) calculations of the lifetimes of the spin-forbidden $2s^2\ ^1S_0$–$2s2p\ ^3P_1$ transition and the spin-allowed $2s^2\ ^1S_0$–$2s2p\ ^1P_1$ transition in Be-like ions have been performed. The importance of the inclusion of the Breit interaction to obtain accurate fine-structure splittings and mixing coefficients is discussed and the noted discrepancy between the length and velocity gauges for the intercombination line in the lighter ions is addressed. Different optimization procedures are evaluated. For C III the experimental intercombination transition rate has been measured to be 121.9 s^{-1} with an accuracy of 6%. The current calculation gives $100.3 \pm 4.0\ s^{-1}$, in agreement with other recent calculations.

PACS number(s): 32.70.Cs, 31.25.Eb, 31.25.Jf

I. INTRODUCTION

Intercombination lines are of great astronomical interest since they constitute accurate diagnostic tools for stellar atmospheres. The 1909-Å line in C III is such an example. It corresponds to the transition $2s^2\ ^1S_0-2s2p\ ^3P_1$, and is frequently found in the spectra of a wide range of astronomical objects. Recent experimental results for the C III ion [1] have stimulated a number of theoretical investigations in this area [2,3]. Conditions similar to those found in the astronomical objects can be produced in the plasmas used in fusion research. In performing plasma diagnostics and tracing impurities it is important to have a detailed knowledge of the spectra of the elements involved. Fe is one of these impurities and is frequently used for diagnostic purposes. Both the resonance line and the intercombination line in the Be-like Fe ion have been observed in, for example, the Princeton Large Torus tokamak plasma [4].

The isoelectronic sequence of the Be-like ions has been the subject of several studies over the past two decades. Most of these studies have employed nonrelativistic approaches and added on the effects of relativity perturbatively through a Breit-Pauli procedure. However, the term dependence of the $2p$ orbital needs to be taken into account before accurate results can be obtained. This leads to an increased complexity of the calculations.

The spin-forbidden intercombination transition is induced by a small configuration mixing of the $2s2p\ ^3P_1$ and the $2s2p\ ^1P_1$ states. This is a purely relativistic effect. It is therefore expected that a Breit-Pauli-type calculation will be valid only for ions with relatively low values of the nuclear charge. The present calculation is based on the fully relativistic Dirac Hamiltonian and therefore will not suffer from this limitation. The calculation is performed stepwise to ensure the convergence for each of the employed models and also to facilitate accurate error estimates. It is expected that the importance of the electron-electron correlation will decrease for the more highly charged ions, which will therefore exhibit a faster convergence. In this paper we will present calculations for the following ions along the isoelectronic sequence: C III, N IV, O V, Si XI, Fe XXIII, amd Mo XXXIX.

II. THEORETICAL BACKGROUND

The multiconfigurational Dirac-Fock (MCDF) calculations were performed using the General Relativistic Atomic Structure Package (GRASP) [5], which has been modified at Vanderbilt University [6] (referred to as GRASP92) to facilitate large-scale computations through the use of dynamic memory allocation and improved convergence features. In a multiconfiguration calculation the atomic state function (ASF) is expanded in terms of a set of configuration state functions (CSF's)

$$\Psi(\gamma PJM) = \sum_i c_i \phi_i(\gamma_i PJM). \tag{1}$$

The CSF's, in a relativistic calculation, are the antisymmetrized sum of products of Dirac spinors. Both the Dirac spinors and the expansion coefficients, as described in the literature [7,8], are optimized to self-consistency for a stationary energy. In an extended optimal level calculation the expression for this energy contains weighted contributions from several levels that are to be investigated.

A. Nonrelativistic approach

In a nonrelativistic calculation the CSF's are normally coupled using the LS term scheme since the nonrelativis-

*Electronic address: ynnerman@vuse.vanderbilt.edu
†Electronic address: cff@vuse.vanderbilt.edu

tic Hamiltonian is diagonal in this representation and consequently only CSF's with the same LS terms will appear in the expansion in Eq. (1). When relativistic effects are taken into account, as in a Breit-Pauli calculation, the Hamiltonian is only diagonal in the total angular momentum J and it is then common to couple the LS terms to LSJ states. As long as the effects of relativity are small, the addition of the J-dependent relativistic interactions cause only small mixings of states from different LS terms and the ASF has one dominating LSJ coupled CSF. In the calculation of the $^1S_0 - {}^3P_1^o$ transition it is the mixing between the $^3P_1^o$ and $^1P_1^o$ levels, together with a smaller mixing of the $2p^2\ {}^3P_0^e$ state and the ground state, that gives rise to the observed $E1$ transition. As long as the mixing between the $^3P_1^o$ and $^1P_1^o$ levels remains comparatively small, it can be assumed that the Breit-Pauli approximation is valid and a reliable value of the intercombination lifetime can be extracted using a nonrelativistic formalism. This type of calculation has been performed for the C III ion, for example, by Froese Fischer [2] and Fleming *et al.* [3]. One of the main problems in these calculations is the necessity to accurately represent the $^1P^o$ term and splitting between the $^1P_1^o$ and $^3P_1^o$ levels. At the Hartree-Fock level, it is well known that the $2p$ state of $^1P^o$ term is much more diffuse than the $2p$ state of the $^3P^o$ term. Correlation orbitals optimized on the $^3P^o$ term will not constitute a good basis for this diffuse behavior. In the previously mentioned systematic Breit-Pauli calculation, one additional orbital of each symmetry was used to supplement the $^3P^o$ basis at each stage and capture this term dependence. A similar technique was used for the $2p^2\ {}^3P$ wave function expansion. This increased the complexity of the calculation considerably. It was our hope that in a relativistic calculation, the term dependence would not appear, or at least not affect the calculation seriously, so that a more simple optimization scheme could be applied.

B. Relativistic approach

In a relativistic calculation the spin and orbital angular momenta for each individual electron are already coupled. This means that the number of relativistic spin orbitals is larger and the number of relativistic CSF's will grow much more rapidly than in the nonrelativistic case.

In the following discussion of the mixing coefficients and the Breit interaction we will limit the expansion of the excited states to the four CSF's that can be formed from the $1s^2_{1/2}2s_{1/2}2p_{1/2}$ and the $1s^2_{1/2}2s_{1/2}2p_{3/2}$ configurations. We have, introducing shorthand notation,

$$\begin{aligned} |\,1\rangle &= |\,1s^2 2s_{1/2}2p_{1/2}, J=0\rangle, \\ |\,2\rangle &= |\,1s^2 2s_{1/2}2p_{1/2}, J=1\rangle, \\ |\,3\rangle &= |\,1s^2 2s_{1/2}2p_{3/2}, J=1\rangle, \\ |\,4\rangle &= |\,1s^2 2s_{1/2}2p_{3/2}, J=2\rangle. \end{aligned} \tag{2}$$

The interaction matrix between these CSF's will contain off-diagonal contributions between the two J=1 states:

$$\begin{pmatrix} \langle 1\,|\,H\,|\,1\rangle & 0 & 0 & 0 \\ 0 & \langle 2\,|\,H\,|\,2\rangle & \langle 2\,|\,H\,|\,3\rangle & 0 \\ 0 & \langle 3\,|\,H\,|\,2\rangle & \langle 3\,|\,H\,|\,3\rangle & 0 \\ 0 & 0 & 0 & \langle 4\,|\,H\,|\,4\rangle \end{pmatrix} \tag{3}$$

and we will thus get a mixing of the J=1 states. In the case of C III the energy separation of the zeroth-order energies for the states are of the order of 0.10 a.u., while the off-diagonal value is 0.13 a.u. This indicates a very strong interaction between the J=1 levels. On the left-hand side of Fig. 1, the energies of the zeroth-order CSF's, i.e., the diagonal elements of the matrix, are shown. It should be noted that the energy scale in the dotted box is enhanced by a factor of 600. The J=2 and J=0 states are very close and the two J=1 states are well above in energy. The interaction between the two J=1 levels causes them to mix and produce two levels much farther apart from each other. One of them belongs to the fine structure of the nonrelativistic $^3P^o$ term and the other one constitutes the $^1P^o$ term. We can write this as

$$\begin{aligned} |\,{}^3P_1^o\rangle &= c_1\,|\,2\rangle + c_2\,|\,3\rangle, \\ |\,{}^1P_1^o\rangle &= c_1\,|\,3\rangle - c_2\,|\,2\rangle. \end{aligned} \tag{4}$$

To represent the fine structure of the $^3P^o$ term it is necessary for the lower of the two J=1 levels to end up in between the J=0 and J=2 levels. In the nonrelativistic limit the mixing of the two levels is entirely due to the angular coupling and the J=0 and J=2 levels become degenerate. The correction due to the relativistic effects enters only through the difference in the shape of the radial parts of the $2p_{1/2}$ and $2p_{3/2}$ orbitals. The mixing and splitting of the levels depend crucially on the shape of these two radial functions. The accuracy of the fine-structure splitting of the $^3P^o$ term is thus a measure of the accuracy of the mixing of the J=1 levels. The problem of the accuracy of the mixing coefficients is now apparent. The interaction of the levels must be able to reflect a fine-structure splitting three orders of magnitude smaller than the eigenenergies of the matrix. Very small relative changes of the values in the matrix in Eq. (3) will affect the fine-structure splitting and the mixing coefficients.

In a MCDF calculation there is a choice of optimization procedures. The most straightforward way would of course be to optimize only on the states involved in the transition in independent calculations. This would, however, produce two sets of nonorthogonal orbitals. The current implementation of the GRASP code does not accommodate this and it is necessary to obtain both the initial and final states of the transition using the same set of orthogonal orbitals. The first choice would then be to optimize the energies for either the initial or the final state. A test run in which optimization was performed only on the initial state was performed and the results for the C III ion are shown in Table I. As can be seen, the fine-structure splitting and the transition rate for the intercombination line exhibit a nonconverging behavior when the effects of core polarization are added. For a discussion of the different computational models used, see Sec. IV. Also, when only the outer correlation effects

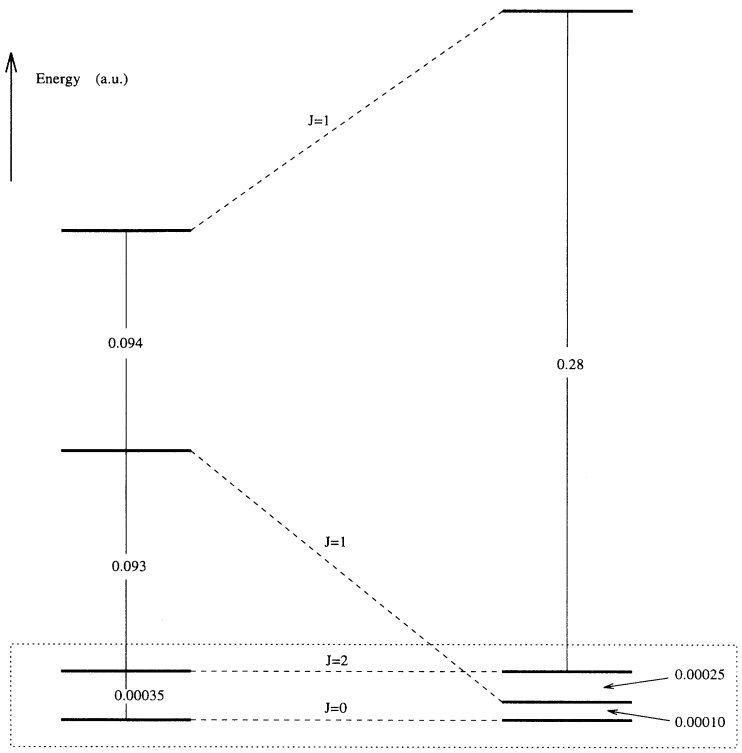

FIG. 1. The levels of the $1s^2 2s2p$ configuration in C III. On the left-hand-side, the energies of the JJ coupled CSF's are given. On the right-hand side, the eigenenergies of the Hamiltonian matrix in Eq. (3) are shown. Inside the dotted box, the energy scale is multiplied by a factor of 600.

are used the convergence of the A factor is poor. A similar behavior was found in the cases when optimization was performed only on the final state and when both the initial and final states were optimized upon simultaneously. It should be noted that all the term energies and the oscillator strength for the resonance line are in good agreement with the experimental values. When an optimization procedure including all the components of the $^3P^o$ term is applied the problem is overcome and the fine-structure exhibits a convergent behavior. As can be seen in Table III, the fine-structure and the transition rate for the intercombination line are now showing a convergent behavior even when core polarization is taken into account.

Taking the above into consideration, it is realized that in any given truncation scheme or variational procedure it is necessary to treat all the levels in the $^3P^o$ term on an equal basis to ensure that the fine-structure is well

TABLE I. The transition energies for the $^1S_0 - ^3P_1^o$, and $^1S_0 - ^1P_1^o$ transitions and the fine-structure splitting of the $^3P^o$ level in C III. Optimization was performed only on the $^3P_1^o$ level. The last four columns give the transition rates for the intercombination and resonance lines for the length and velocity gauges.

	Energy (cm^{-1})						Transition rate (s^{-1})		Oscillator strength	
	$^1S_0$-$^3P_1^o$	$^3P_0^o$-$^3P_1^o$	$^3P_1^o$-$^3P_2^o$	$^3P_0^o$-$^3P_2^o$	$^1S_0$-$^1P_1^o$	$^3P_1^o$-$^1P_1^o$	$(^3P_1^o - ^1S_0)_l$	$(^3P_1^o - ^1S_0)_v$	$(^1P_1^o - ^1S_0)_l$	$(^1P_1^o - ^1S_0)_v$
					Calculation					
Outer correlation										
n=2	53430.64	22.202	54.211	76.413	115286.3	61855.7	53.46	1.3	0.68120	0.68590
n=3	53393.00	22.166	53.764	75.930	113378.6	59985.6	52.81	0.9	0.68766	0.69237
n=4	52617.95	23.478	55.879	79.357	103957.5	51339.6	77.72	56.70	0.75940	0.83962
n=5	52702.84	22.859	54.494	77.353	103745.6	51042.8	94.51	102.3	0.76527	0.84514
n=6	52725.21	22.740	54.353	77.093	103682.7	50957.5	96.91	125.45	0.76667	0.84472
n=7	52731.97	22.714	54.295	77.009	103665.3	50933.3	100.64	105.25	0.76708	0.84469
n=8	52738.09	22.713	54.289	77.002	103644.9	50906.8	94.92	121.97	0.76803	0.84559
Core polarization										
n=2	53497.37	22.707	55.238	77.945	115202.4	61705.0	149.26	4341	0.67901	0.65297
n=3	52625.98	50.930	113.15	164.08	111858.5	59232.8	1522	13830	0.67436	0.60188
n=4	52089.22	36.883	88.713	125.60	104043.0	51953.8	1470	1915	0.72461	0.71776
n=5	52194.06	23.692	62.803	86.495	103320.8	51126.7	267.42	239.64	0.72309	0.71825
					Experiment[a]					
	52390.75	23.69	56.36	80.05	102352.0	49961.3	120.9±7.0[b]		0.754±0.014[c]	

[a]Moore, Ref. [19].
[b]Kwong *et al.*, Ref. [1].
[c]Reistad and Martinson, Ref. [15].

represented, thereby also obtaining physically correct $2p$ orbitals. In a situation where an optimization would be performed only on the $J=1$ levels, the energy of the $^3P_1^o$ term is overemphasized and the fine-structure splitting will be poorly represented. This is reflected in nonphysical $2p$ orbitals and mixing coefficients.

As the value of the nuclear charge Z is increased the fine-structure splitting will increase and the difference between the two $2p$ orbitals will be more distinct, giving a smaller mixing of the $J=1$ levels. Thus the JJ coupled zeroth-order CSF's will be a better representation of the physical situation for high-Z ions. The concept of $^3P^o$ and $^1P^o$ terms is then no longer applicable.

C. Breit interaction

In the variational relativistic procedure adopted here the frequency-independent Breit interaction is not included, even though the conceptual problems of such a procedure must now be assumed overcome [9]. The effect of the transverse Breit interaction can thus only be included in a configuration-interaction (CI) calculation using the variationally obtained relativistic spin orbitals. The effect of the Breit operator in a light ion such as C III is very small indeed. The importance of a proper account of this interaction can be found in the conclusion of Sec. II B Small relative changes of the elements of the matrix in Eq. (3) will produce large relative changes of the fine-structure, thereby also affecting the mixing coefficients. The contribution of the Breit interaction increases the energy of the diagonal elements and introduces small relative changes of the order 10^{-4} a.u., which is enough to have a dramatic impact on the fine-structure splitting. As an example of this effect, we show in Table II calculations for C III with and without the Breit interaction. As can be seen, the Breit interaction affects the fine-structure splitting by almost 50% and the value for the intercombination line transition rate is thus seriously affected. The fine-structure splitting scales as Z^4, whereas the Breit interaction shows a Z^2 dependence. The relative importance of this effect is therefore, counter intuitively, decreasing with Z, making the inclusion of the Breit interaction more important for the lighter elements, a behavior that was confirmed during the calculation of the isoelectronic sequence. The importance of the inclusion of the Breit interaction in calculations of intercombination line strengths was noted, but not explained in detail, in a recent calculation on P II by Fritzsche and Grant [10]. Also previous Breit-Pauli calculations have accommodated the major parts of the Breit interaction through the inclusion of spin-spin and spin-other-orbit terms [11,12]. For the lightest elements considered in this paper it is even possible that higher orders of the Breit interaction may have a nonvanishing effect, thereby setting a limit to the accuracy of the present calculation for these cases.

D. Gauge dependence

In a calculation of an electric dipole transition it is the matrix element of the electric dipole operator that is sought. There are two different choices of forms of the dipole operator: the velocity form, which is based on the expectation value of the gradient operator, and the length form, in which the expectation value of $\boldsymbol{r}$ is used. The two gauges are related through the difference in energy ΔE between the initial and final state as

$$\langle \Psi_f \mid \boldsymbol{\nabla} \mid \Psi_i \rangle = \Delta E \langle \Psi_f \mid \boldsymbol{r} \mid \Psi_i \rangle. \tag{5}$$

If we insert the expansion of the initial state Eq. (4), into the expressions we get, using the shorthand notation introduced in Eq. (2),

$$c_1 \langle \Psi_f \mid \boldsymbol{\nabla} \mid 2 \rangle + c_2 \langle \Psi_f \mid \boldsymbol{\nabla} \mid 3 \rangle = \Delta E \left(c_1 \langle \Psi_f \mid \boldsymbol{r} \mid 2 \rangle + c_2 \langle \Psi_f \mid \boldsymbol{r} \mid 3 \rangle \right). \tag{6}$$

In the case of C III the allowed transition, which is obtained by exchanging the coefficients c_1 and c_2, has an A factor of the order 10^9 s^{-1}, whereas the intercombination line is of the order 10^2 s^{-1}. This means that the individual matrix elements must be of the order 10^4 and in the case of the intercombination line there must be a cancellation of at least three orders of magnitude between the products of the matrix elements and the expansion coefficients. The numerical problems involved with these calculations have been addressed by Ellis [13]. It is a well-known fact that the inaccuracy in the velocity form for a given truncation scheme is larger than that for the

TABLE II. Test of the importance of the Breit interaction in the calculation of the intercombination line transition rate for C III. The $n=4$ limit for the core polarization in the full optimization scheme was used.

	Energy (cm^{-1})						Transition rate (s^{-1})		Oscillator strength	
	$^1S_0$-$^3P_1^o$	$^3P_0^o$-$^3P_1^o$	$^3P_1^o$-$^3P_2^o$	$^3P_0^o$-$^3P_2^o$	$^1S_0$-$^1P_1^o$	$^3P_1^o$-$^1P_1^o$	$(^3P_1^o$-$^1S_0)_l$	$(^3P_1^o$-$^1S_0)_v$	$(^1P_1^o$-$^1S_0)_l$	$(^1P_1^o$-$^1S_0)_v$
					Calculation					
Core polarization										
n=4 (no Breit)	52119.70	32.710	70.168	102.88	102956.2	50836.5	131.5	121.7	0.75755	0.76763
n=4 (Breit)	52120.35	21.458	56.867	78.325	102948.4	50828.1	99.90	188.2	0.75767	0.76810
					Experiment[a]					
	52390.75	23.69	56.36	80.05	102352.0	49961.3	120.9±7.0[b]		0.754±0.014[c]	

[a]Moore, Ref. [19].
[b]Kwong *et al.*, Ref. [1].
[c]Reistad and Martinson, Ref. [15].

length form. This is due to the fact that the two forms are sensitive to different regions of the wave function. In a variational calculation the wave functions are optimized on an energy expression. This will give a relatively better representation of the outer part of the wave functions and thus favor the length form. It is also clear from Eq. (6) that the velocity gauge implicitly contains a dependence on the transition energy in the matrix element, which may affect the accuracy of the evaluation. Due to the above given reasons, a much slower convergence of the velocity gauge is expected.

As the nuclear charge increases, the A factor for the intercombination line will increase drastically as the seventh power of the nuclear charge for the lighter ions. This is due to the increased size of the relativistic effects and the more pure representation in terms of JJ coupling. The resonance line will exhibit a small linear Z dependence. This means that the cancellation of the terms will decrease and the demand on the accuracy is lowered. A faster convergence is therefore anticipated for the heavier ions in the isoelectronic sequence.

III. METHOD OF CALCULATION

The GRASP code does not accommodate the use of nonorthogonal orbitals. This means that the same set of spin orbitals must be used in the expansion of both the odd parity and even parity levels involved in the $E1$ transition. There are in principle two different ways of allowing the calculation to minimize the energy. The average level type calculation uses the weighted sum of the diagonal Hamiltonian matrix elements for the levels specified. The optimal level (OL) scheme minimizes the energy for one level. The OL scheme can be extended to include several levels in an energy functional that contains weights for the levels under consideration, this is referred to as an extended optimal level (EOL) calculation.

The first and most straightforward way of performing a calculation for the intercombination lifetime, given the restriction of the GRASP code, would be to use the EOL procedure and optimize on the $^1S_0$, $^3P^o_1$, and $^1P^o_1$ levels. As pointed out in Sec. II B, this approach will produce nonphysical $2p$ orbitals at a given truncation scheme and consequently the results of the calculation can be orders of magnitude off. The remedy is to include all the components of the $^3P^o$ term in the optimization procedure.

At the same time it is important to appreciate the fact that the same spin orbitals are used to represent very different states of the atom. It has been noticed [2] that nonrelativistic orbitals may show a very strong *term-dependence*; see Sec. II A. For instance, the p orbital of the $^3P^o$ term is very different from the p orbital obtained when optimizing on the $^1P^o$ term. Also the shapes of the orbitals differ between the initial and final states of the transition. To include the possible effects of this dependence, a scheme was designed in which active set expansions were used to generate the CSF's for cases were the principal quantum number n was truncated at a given value. For n=2,3 the energy functional contained only contributions from the $^3P^o$ term. The orbitals were then fixed and for n=4 the energy was optimized for the $^1P^o$ term and for the n=5 limit the spin orbitals were optimized for the ^1S term. Since node counting was not enforced for any of the correlation spin orbitals, it is assumed that the term dependence was represented through this procedure. The scheme was then repeated until reliable limiting values could be extracted.

Two different types of active set expansions were used. The first one including only the effect of the *outer correlation*, i.e., constructing all the CSF's possible by substituting the two $2s$ electrons for the initial state and the $2s2p$ electrons for the final state. To include the effect of core polarization, the second type of active set expansion allowed also one of the $1s$ electrons to be replaced. In this way, outer correlation and core polarization were treated on the same footing. In all the active sets the orbital angular momentum of the individual electrons were limited to s, p, d, and f symmetries.

As shown in Sec. II C, the inclusion of the Breit interaction turned out to be one of the important steps for the correct representation of the fine-structure splitting, thereby also of reliable mixing coefficients. In GRASP the Breit interaction cannot be treated self-consistently. For each active set a CI procedure, using the variationally obtained spin orbitals, was used to evaluate the contribution from the exchange of one transverse virtual photon.

The effect of some selected triple and quadruple excitations was also evaluated in the CI calculation. All possible excitations that can be formed within the n=3 limit were included. The n=4 quadruples turned out to produce configuration lists that were not possible to include at this stage.

IV. RESULTS

Extensive investigations of the C III ion have taken place over the past several years. Both experimental and theoretical values have been produced with increasing accuracy. For the isoelectronic sequence there is little or no data available in the literature. The following discussion therefore focuses the comparison of the results on the C III case and gives a more general discussion of the isoelectronic calculations.

A. C III

In Table III the transition energies and fine-structure splittings are given for the C III ion. The scheme outlined in Sec. III, was used to obtain the limiting values for the three different models. For the outer correlation only the limiting values of the transition energies, for both the resonance line and the intercombination line, lie within 1.5% of the experimental values. When core polarization is included, the calculated value agrees with experiment to the 0.01% level for the intercombination transition and to 0.3% for the resonance transition. The inclusion of the triple and quadruple excitations makes the agreement slightly worse, indicating the greater difficulty in

TABLE III. The transition energies for the $^1S_0$-$^3P_1^o$, and $^1S_0$-$^1P_1^o$ transitions and the fine-structure splitting of the $^3P^o$ in C III. The values for the transition rate for the intercombination line and the oscillator strength for the resonance transition are given in the last four columns. The optimization was performed on all the components of the $^3P^o$, $^1P^o$, and ^1S terms as described in the text.

	Energy (cm^{-1})						Transition rate (s^{-1})		Oscillator strength	
	$^1S_0$-$^3P_1^o$	$^3P_0^o$-$^3P_1^o$	$^3P_1^o$-$^3P_2^o$	$^3P_0^o$-$^3P_2^o$	$^1S_0$-$^1P_1^o$	$^3P_1^o$-$^1P_1^o$	$\left(^3P_1^o - {}^1S_0\right)_l$	$\left(^3P_1^o - {}^1S_0\right)_v$	$\left(^1P_1^o - {}^1S_0\right)_l$	$\left(^1P_1^o - {}^1S_0\right)_v$
					Calculation					
Outer Correlation										
n=2	53452.62	22.202	54.210	76.412	115285.5	61832.9	46.7	0.5	0.68122	0.68604
n=3	53443.83	22.436	54.342	76.778	114219.5	60775.7	46.6	6.7	0.68273	0.68635
n=4	52683.27	22.650	54.256	76.906	103818.0	51134.7	90.7	128.2	0.76746	0.84595
n=5	52723.98	22.676	54.256	76.932	103693.3	50969.3	91.7	130.3	0.76847	0.84670
n=6	52729.80	22.698	54.264	76.962	103657.8	50928.0	91.8	132.2	0.76838	0.84578
n=7	52732.91	22.695	54.261	76.956	103688.3	50955.4	91.7	133.3	0.76851	0.84643
n=8	52717.66	22.701	54.272	76.973	103633.1	50915.4	92.3	138.3	0.76889	0.84712
Core polarization										
n=2	53507.85	22.167	54.146	76.313	115215.0	61707.2	46.0	60.1	0.67924	0.65717
n=3	52630.20	22.697	56.242	78.939	111727.5	59097.3	59.3	60.2	0.67511	0.60471
n=4	52120.35	21.458	56.867	78.325	102948.4	50828.1	99.9	188.2	0.75767	0.76810
n=5	52291.09	20.999	57.290	78.289	102926.1	50635.0	108.4	184.4	0.75681	0.76051
n=6	52349.00	21.202	57.829	79.031	102870.8	50521.8	114.7	233.3	0.75724	0.75536
n=7	52382.41	21.026	57.641	78.667	102724.3	50341.9	104.8	173.7	0.76029	0.75479
n=8	52370.09	21.071	57.621	78.692	102765.0	50394.9	103.4	170.2	0.76023	0.75503
n=9	52398.97	21.023	57.674	78.697	102732.2	50333.2	103.8	170.5	0.76037	0.75484
Selected triples and quadruples										
n=6	52327.96	21.654	57.216	78.870	102867.0	50539.0	111.2	236.4	0.75411	0.75408
n=7	52360.61	21.483	57.036	78.519	102723.1	50362.5	101.7	178.1	0.75699	0.75331
n=8	52372.19	21.490	57.067	78.557	102725.6	50353.4	100.3	174.3	0.75705	0.75330
					Experiment[a]					
	52390.75	23.69	56.36	80.05	102352.0	49961.3	120.9±7.0[b]		0.754±0.014[c]	

[a]Moore, Ref. [19].
[b]Kwong *et al.*, Ref. [1].
[c]Reistad and Martinson, Ref. [15].

performing a systematic calculation involving triples and quadruples. The fine-structure splitting exhibits a very stable behavior as the calculation is expanded. The inclusion of the core polarization and the triple and quadruple excitations affect the splittings significantly and are thus, as discussed in Sec. II B, important to include in order to represent the fine-structure. The converged values are, however, slightly below the experimental ones. This was also the case in the Breit-Pauli calculations by Froese Fischer [2] and Fleming *et al* [3]. In the latter a fine tuning of the fine-structure splitting was used to obtain better mixing coefficients and thereby eliminate the errors introduced by the inaccuracy in the *ab initio* calculated values. It is our suspicion that this noted discrepancy may be due to neglected higher orders of the Breit interaction.

In Table III the transition rate for the intercombination line and the weighted oscillator strength for the resonance line are given for the different models and truncation limits. The value for the intercombination line, calculated in the outer correlation only model, was assumed to have converged at the n=8 limit at 92 s^{-1}. Adding the core polarization increased the value significantly and finally the introduction of the triples and quadruples gave the final value 100.3 ± 4.0 s^{-1}. The error was estimated by a comparison of the convergence of the different models and by comparing the theoretical transition energies and fine-structure splittings with the experimental values. There is a large difference in the values obtained using the length and velocity forms of the dipole operator. As discussed in Sec. II D, this is due to the high demand of the accuracy of the terms that contribute in the cancellation between two allowed transition matrix elements. Also the fact that the two forms are sensitive to different regions of the wave function may explain the difference. In our procedure the wave functions are optimized on an energy expression. This will implicitly favor the accuracy of the length form.

In Table IX experimental and other calculated values for the intercombination transition are given. The only previous MCDF calculation is the one by Cheng *et al.* [14], in which the calculation was limited to the n=2 complex and clearly cannot compete with the much more elaborate calculation presented here. The more recent calculations, using the Breit-Pauli approximation, give values very close to the one obtained here. It is evident from the convergence of the calculation (see Table III) that the present calculation is one of the most accurate to date and that the MCDF approach is able to produce reliable results for intercombination lines even in low-Z ions. The experimental value, obtained using a radio-frequency ion trap [1], is significantly larger than any of the theoretical values and well outside the estimated errors. In this case, theory seems to agree and the most probable cause of the discrepancy must lie on the experimental side.

As discussed in Sec. II B, the allowed transition between the $2s^2$ $^1S_0$ and $2s2p$ $^1P_1^o$ states is spin allowed, and therefore dominated by nonrelativistic effects, and there is no need to add the Breit-Pauli terms to a nonrelativistic calculation to obtain a value for the oscillator strength. There are a number of previous evaluations of

the oscillator strength for this transition. A more complete account for the theoretical history can be found in Refs. [2,3]. The most recent values are, however, given in Table X. In the present calculation all the effects of relativity were implicitly taken into account, even though they may not have any effect on the oscillator strength for low-Z ions such as C III.

The present calculation is in very close agreement with other recent theoretical values. The experimental value given by Reistad and Martinson [15] is somewhat lower than the theoretical ones, but with the estimated error taken into account it lies within the theoretical range.

B. Isoelectronic sequence

The methods applied to the C III calculation were repeated for a number of selected ions along the isoelectronic sequence. The selected ions were N IV (Table IV), O V (Table V), Si XI (Table VI), Fe XXXIII (Table VII), and Mo XXXXIX (Table VIII). The calculations were limited polarization models and the inclusion of the triple and quadruple excitations in the n=3 limit, as described above. Only for the Mo ion was the outer correlation only model applied to investigate the importance of the core polarization effects for the highly ionized ions.

As expected, the convergence of the transition rate for the intercombination line is significantly improved as the value of Z increases. As described in Sec. II B, this is due to the fact that the JJ coupling scheme is an increasingly better description of the system and the relative importance of the Breit interaction decreases as the fine-structure splitting increases. It was found that for the Mo ion the convergence to two significant numbers was achieved already at the n=5 level, whereas for the N IV ion the calculation had to be taken to the n=8 limit to obtain the same level of accuracy. Also the effects of core polarization and the triple and quadruple excitations were found to be less important for the heavier ions.

The noted difference between the length and velocity forms of the dipole operator is also decreasing, as discussed in Sec. II D. The relative difference between the gauges is 73% for the C III ion, 39% for O V, and only 2% for Mo. For the lighter ions the A factor shows a clear Z^7 dependence. As the transition rate grows with Z, the dependence changes. This is due to the fact that the cancellation of the terms in Eq. (6) is now reduced and the transition rate is approaching the actual values of the individual matrix elements, i.e., the transition becomes saturated. It is therefore expected that in the limit the heavier ions will exhibit the Z^4 dependence of an allowed transition. To verify this behavior $\log_{10}(A)/\log_{10}(Z)$ was plotted as function of $1/Z$ and the data points were fitted to splines; see Fig. 2. The intersection with the y-axis would give the Z-dependence for a nucleus with infinite charge. The results obtained by Cheng *et al.* [14] in a very restricted MCDF calculation, including only the CSF's obtained from the n=2 limit, have been included as the solid line in the plot.

In Table IX a comparison with experimental values and other calculations is given. Experimental data are only available for C III and Fe XXIII. Alas the error associated with the Fe XXIII ion is too large to facilitate any critical evaluation of the accuracy of the value obtained in the present calculation. For C III there are many other calculations. We have, however, concentrated here on the isoelectronic sequence calculations and chosen to give only the most recent values for the lighter elements. A full presentation of the C III case can be found in Refs. [2,3]. It is clear that the accuracy of the present calculation is higher even for the low-Z ions. It would be interesting

TABLE IV. The transition rate for the $^1S_0$-$^3P_1^o$ transition and the weighted oscillator strength for the $^1S_0$-$^1P_1^o$ transition in N IV. The quadruple excitations were limited to the $n < 4$ orbitals.

	$^1S_0$-$^3P_1^o$			$^1S_0$-$^1P_1^o$		
		$A\,(\mathrm{s}^{-1})$			gf	
	ΔE	Length	Velocity	ΔE	Length	Velocity
			Calculation			
Core polarization						
n=2	68481.1	313.4	15.5	144080	0.56484	0.53546
n=3	67506.8	373.8	289.8	140217	0.56033	0.49323
n=4	66981.8	552.6	890.7	131375	0.60732	0.61207
n=5	67161.3	569.2	810.5	131345	0.60773	0.60795
n=6	67224.9	568.4	834.4	131294	0.60857	0.60588
n=7	67275.2	574.4	825.9	131135	0.61193	0.60778
n=8	67287.5	576.8	826.6	131142	0.61196	0.60782
Selected triples and quadruples						
n=6	67202.2	556.3	849.4	131273	0.60662	0.60586
n=8	67263.9	564.3	841.3	131122	0.60992	0.60763
			Experiment[a]			
	67272.3			130693		

[a]Moore, Ref. [20].

TABLE V. The transition rate for the $^1S_0$-$^3P_1^o$ transition and the weighted oscillator strength for the $^1S_0$-$^1P_1^o$ transition in O V. The quadruple excitations were limited to the $n < 4$ orbitals.

	$^1S_0$-$^3P_1^o$			$^1S_0$-$^1P_1^o$		
		$A\,(s^{-1} \times 10)$			gf	
	ΔE	Length	Velocity	ΔE	Length	Velocity
			Calculation			
Core polarization						
n=2	83335.1	146.0	18.2	172547	0.482459	0.451732
n=3	82299.4	160.2	111.4	168432	0.478341	0.416932
n=4	81797.0	218.0	322.4	159566	0.507286	0.508193
n=5	81975.9	224.2	298.6	159519	0.508495	0.506942
n=6	82038.0	224.4	301.9	159456	0.509447	0.506202
Selected triples and quadruples						
n=6	82015.4	220.7	306.2	159427	0.508090	0.506565
			Experiment[a]			
	82078.6			158798		

[a]Moore, Ref. [21].

TABLE VI. The transition rate for the $^1S_0$-$^3P_1^o$ transition and the weighted oscillator strength for the $^1S_0$-$^1P_1^o$ transition in Si XI.

	$^1S_0$-$^3P_1^o$			$^1S_0$-$^1P_1^o$		
		$A\,(s^{-1} \times 10^3)$			gf	
	ΔE	Length	Velocity	ΔE	Length	Velocity
			Calculation			
Core polarization						
n=2	173692	286.4	105.9	344605	0.259499	0.237216
n=3	172507	303.7	190.4	339870	0.257695	0.221463
n=4	172239	350.7	387.4	331035	0.262697	0.259428
n=5	172372	353.9	384.5	330930	0.263342	0.260806
n=6	172453	358.6	401.8	330714	0.265045	0.264616
			Experiment[a]			
	172144			329679		

[a]Martin and Zalubas, Ref. [22].

TABLE VII. The transition rate for the $^1S_0$-$^3P_1^o$ transition and the weighted oscillator strength for the $^1S_0$-$^1P_1^o$ transition in Fe XXIII

	$^1S_0$-$^3P_1^o$			$^1S_0$-$^1P_1^o$		
		$A\,(s^{-1} \times 10^5)$			gf	
	ΔE	Length	Velocity	ΔE	Length	Velocity
			Calculation			
Core polarization						
n=2	384052	475.6	264.4	770419	0.153735	0.141384
n=3	382627	486.5	331.8	765474	0.153025	0.133495
n=4	382434	516.7	519.9	756942	0.153969	0.149805
n=5	382591	518.6	522.5	756825	0.154153	0.150555
			Experiment[a]			
	379130			752840		

[a]Shira, Ref. [23].

TABLE VIII. The transition rate for the $^1S_0$-$^3P_1^o$ transition and the weighted oscillator strength for the $^1S_0$-$^1P_1^o$ transition in Mo XXXIX.

	$^1S_0$-$^3P_1^o$			$^1S_0$-$^1P_1^o$		
		$A\,(s^{-1} \times 10^6)$			gf	
	ΔE	Length	Velocity	ΔE	Length	Velocity
			Calculation			
Outer correlation						
n=2	748879	913.7	713.8	2035280	0.140233	0.141671
n=3	750104	912.6	897.4	2036287	0.140092	0.148455
n=4	747240	936.0	1184	2025452	0.140310	0.149795
n=5	747319	937.2	1189	2025350	0.140429	0.150115
Core polarization						
n=2	749001	913.5	601.7	2035072	0.140053	0.135010
n=3	746685	918.3	692.6	2030700	0.139559	0.129433
n=4	745693	934.9	902.0	2023570	0.139689	0.135986
n=5	745924	936.6	920.3	2023642	0.139794	0.136416

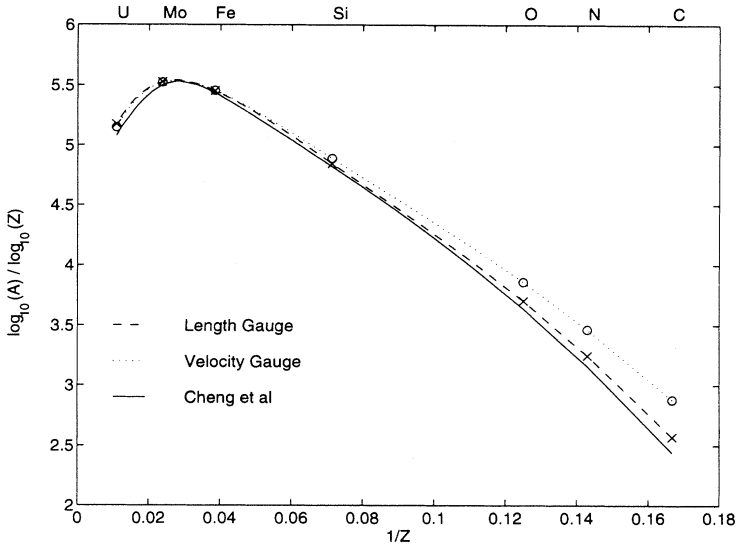

FIG. 2. The $\log_{10}$ of the transition rate divided by $\log_{10}(Z)$ along the isoelectronic sequence plotted as functions of $1/Z$. The dotted and dashed lines are the fitted results from the velocity and length forms of the dipole operator, respectively. The markers show the actual values from the calculation. The solid line represents the results obtained by Cheng *et al.* [14] in a limited MCDF calculation. The limiting value of the Z dependence for large-Z values is obtained as the intersection with the y axis. As discussed in the text, the limiting value should be that of an allowed $E1$ transition, i.e., a Z^4 dependence.

TABLE IX. Comparison of present results for the $2s^2\ ^1S_0$–$2s2p\ ^3P_1$ intercombination line in the Be-like isoelectronic sequence with experiment and other theoretical results.

Ion / Results	C III (s^{-1})	N IV (s^{-1})	O V ($s^{-1} \times 10$)	Si XI ($s^{-1} \times 10^3$)	Fe XXIII ($s^{-1} \times 10^5$)	Mo XXXIX ($s^{-1} \times 10^6$)
Experiment	120.9±7.0[a]			770± 300[b]		
Theory						
Present	100.3±4.0	564.3±4.0	220.7±4.0	358.6±8.0	518.6±4.0	936.6±4.0
Other						
MCHF[c]	103±3					
CI[d]	104±4	495	199	348		
MCDF[e]	79.5	471	193	336	491	841

[a]Kwong *et al.*, Ref. [1].
[b]Dietrich *et al.*, Ref. [24].
[c]Froese Fischer, Ref. [2].
[d]Fleming *et al.*, Ref. [3], obtained using experimental fine-structure splittings; Glass, and Hibbert, Ref. [25]; and Hibbert, Ref. [17].
[e]Cheng *et al.*, Ref. [14].

TABLE X. Comparison of present results for the $2s^2\ ^1S_0$-$2s2p\ ^1P_1$ resonance line in the Be-like isoelectronic sequence with experiment and other theoretical results.

Ion / Results	C III	N IV	O V	Si XI	Fe XXIII	Mo XXXIX
Experiment	0.754(14)[a]	0.619(22)[b]	0.53(2)[b]	0.276(24)[c]	0.150[d]	
Theory						
Present	0.7571(20)	0.6099(20)	0.5081(20)	0.2650(20)	0.1542(10)	0.1398(5)
Other						
MCHF[e]	0.7566(20)					
CI[f]	0.7556	0.618	0.517			
Model potential[g]	0.764	0.614	0.513			
MCDF[h]	0.7942	0.6343	0.5290	0.2705	0.1552	0.1390

[a] Reistad and Martinson, Ref. [15], and Träbert, Ref. [26].
[b]Engström *et al.*, Ref. [27].
[c]Träbert and Heckmann, Ref. [28].
[d]Buchet *et al.*, Ref. [29].
[e]Froese Fischer, Ref. [2].
[f]Fleming *et al.*, Ref. [3], and Glass, Ref. [16].
[g]Laughlin *et al.*, Ref. [18]
[h]Cheng *et al.*, Ref. [14].

to have data from Breit-Pauli type calculations to compare with for the more highly ionized atoms, and thereby verify the limitations of the Breit-Pauli procedure.

Also the oscillator strengths for the allowed transition were calculated for the isoelectronic sequence and compared to available experimental and theoretical data; see Table X. Apart from the MCDF calculation by Cheng *et al.* [14], there are no available results for the high-Z ions. It is striking how well the simple n=2 MCDF calculation agrees with the present values for Fe and MO, showing the decreasing importance of the electron-electron correlation as the nuclear charge increases. In Fig. 3 the oscillator strength has been plotted as a function of $1/Z$ for the two forms of the dipole operator. The agreement is, as expected, excellent for the high-Z ions. The relativistic effects become increasingly important as Z increases and show up as a dramatic increase of the oscillator strength. In the case of C III there are, as discussed above, several independent accurate calculations. For N and O, the calculations by Glass [16] and Hibbert [17] have been combined to produce the CI entry in Table X. Also the model potential calculation by Laughlin *et al.* [18] has been included as a separate entry. There is fair agreement between the present calculation and the other available results. The accuracy of the previous calculations can, however, be questioned.

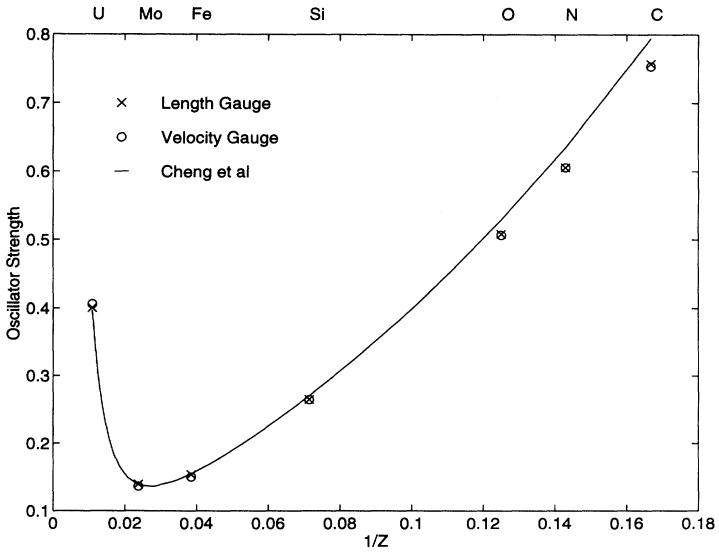

FIG. 3. The oscillator strength for the allowed transition as a function of $1/Z$. The solid line shows the results obtained by Cheng *et al.* [14] in a limited MCDF calculation. The dramatic increase of the oscillator strength for the high-Z ions is due to the increasingly important relativistic effects.

V. CONCLUSION

Systematic MCDF calculations of the intercombination line strength $1s^22s^2\ {}^1S_0 - 1s^22s2p\ {}^3P_1$ in the Be-like isoelectronic sequence have been performed. The resonance transition $1s^22s^2\ {}^1S_0 - 1s^22s2p\ {}^1P_1$ has been evaluated. The systematic approach leads to estimates of the convergence for the properties calculated and reliable error estimates have been possible to determine. The transition energies have also been tabulated and the C III fine-structure splitting has been investigated in some detail.

A theoretical discussion of the problems involved in a relativistic calculation of intercombination line strengths showed the importance of an accurate fine-structure splitting to obtain reliable values of the mixing between the relativistic CSF's. The inclusion of the Breit interaction played an important role in the achievement of the desired accuracy of the fine-structure, especially for the ions with lower nuclear charge. Also the problems involved when using the velocity form of the dipole operator have been addressed.

It is clear that the MCDF approach is able to produce competitive results even for the lighter elements considered in this study. The advantage over the nonrelativistic methods lies, however, in the facilitation of the calculations on the heavier ions, for which the Breit-Pauli approximation used in the nonrelativistic calculations no longer is valid.

ACKNOWLEDGMENTS

The authors wish to thank Dr. Jacek Bieron for many useful discussions and stimulating collaborations on the GRASP94 project. Andreas Stathopoulos has contributed by making adjustments to the Davidson eigenvalue solver during the course of the project. Dr. Farid Parpia is greatly acknowledged for his pioneering work on the GRASP92 code. He also provided valuable initial insights into the required optimization procedures. This research was supported by the Division of Chemical Sciences, Office of Basic Energy Sciences, Office of Energy Research, U.S. Department of Energy.

[1] H. S. Kwong *et al.*, Astrophys. J. **411**, 431 (1993).
[2] C. Froese Fischer, Phys. Scr. **49**, 323 (1994).
[3] J. Fleming, A. Hibbert, and R. P. Stafford, Phys. Scr. **49**, 316 (1994).
[4] J. H. Davé *et al.*, J. Opt. Soc. Am. B **4**, 635 (1987).
[5] K. G. Dyall *et al.*, Comput. Phys. Commun. **55**, 425 (1989).
[6] F. A. Parpia, C. F. Fischer, and I. P. Grant (unpublished).
[7] I. P. Grant *et al.*, Comput. Phys. Commun. **21**, 207 (1980).
[8] C. Froese Fischer, *The Hartree-Fock Method for Atoms* (Wiley, New York, 1977).
[9] E. Lindroth, A.-M. Mårtensson-Pendrill, A. Ynnerman, and P. Öster, J. Phys. B **22**, 2447 (1989).
[10] S. Fritzsche and I. P. Grant, Phys. Lett. A **186**, 152 (1994).
[11] T. Brage, G. Merkelis, and C. F. Fischer, Phys. Lett. A **174**, 111 (1993).
[12] T. Brage and C. F. Fischer, Phys. Scr. **47**, 18 (1993).
[13] D. G. Ellis, Phys. Scr. **40**, 12 (1989).
[14] K. T. Cheng, Y.-K. Kim, and J. P. Desclaux, At. Data Nucl. Data Tables **24**, 111 (1979).
[15] N. Reistad and I. Martinson, Phys. Rev. A **34**, 2632 (1986).
[16] R. Glass, J. Phys. B **12**, 1633 (1979).
[17] A. Hibbert, J. Phys. B **13**, 1721 (1980).
[18] C. Laughlin, E. R. Constantinides, and G. A. Victor, J. Phys. B **11**, 2243 (1978).
[19] C. E. Moore, *Selected Tables of Atomic Spectra C* I–VI, NBS-3 (U.S. GPO, Washington, DC, 1970), Sec. 3.
[20] C. E. Moore, *Selected Tables of Atomic Spectra, N* IV–VII, NBS-3 (U.S. GPO, Washington, DC, 1971), Sec. 4.
[21] C. E. Moore, *Selected Tables of Atomic Spectra, O* V, NBS-3 (U.S. GPO, Washington, DC, 1980), Sec. 9.
[22] W. C. Martin and R. Zalubas, J. Phys. Chem. Ref. Data **12**, 323 (1983).
[23] T. Shira, J. Phys. Chem. Ref. Data **19**, 127 (1990).
[24] D. D. Dietrich *et al.*, Phys. Rev. A **18**, 208 (1978).
[25] R. Glass and A. Hibbert, J. Phys. B **11**, 2413 (1978).
[26] E. Träbert, Z. Phys. D **9**, 143 (1988).
[27] L. Engström *et al.*, Phys. Scr. **24**, 551 (1981).
[28] E. Träbert and P. H. Heckmann, Phys. Scr. **22**, 489 (1980).
[29] J. B. Buchet *et al.*, Phys. Rev. A **30**, 309 (1984).